Cohesive properties of the lanthanides: Effect of generalized gradient corrections and crystal structure

Anna Delin, Lars Fast, and Börje Johansson

Condensed Matter Theory Group, Department of Physics, Uppsala University, P.O. Box 530, S-75121 Uppsala, Sweden

Olle Eriksson and J. M. Wills

Center for Materials Science and Theoretical Division, Los Alamos National Laboratory, Los Alamos, New Mexico 87544

(Received 10 November 1997)

Two different approximations to the density functional, the local (spin) density approximation (LDA) in the Hedin-Lundqvist parametrization and the Perdew-Wang generalized gradient approximation (GGA), are compared using the lanthanide series plus barium as testing ground. Our total-energy calculations are parameter-free and all-electron, with a full-potential linear muffin-tin orbital basis set. The equilibrium volumes, bulk moduli, and generalized cohesive energies are calculated, assuming both the fcc and hcp crystal structures, and compared to experimental data. We find that GGA corrects most of the overbonding tendency of LDA for these elements. Our results also suggest that the standard model of the lanthanides, according to which the $4f$ shell can be viewed as chemically inert, is not fully appropriate for the early lanthanides (not including La), and that the trend in the bulk modulus is much less smooth than previously thought. [S0163-1829(98)00331-2]

I. INTRODUCTION

Ground-state properties of solids can, in principle, be calculated exactly within the framework of density-functional theory (DFT).[1,2] However, on the road from principle to practice, a number of approximations have to be invoked. A common approximation made is that the electron density is only slowly varying. One can then make use of the local (spin) density approximation (LDA),[2] which is exact when the electron density is uniform. Although this is seemingly a very crude approximation, LDA has been widely applied to solids and proven to be very successful in the past. Nevertheless, many attempts have been made to improve upon the LDA. Of the many nonlocal functionals that have been suggested, the one developed by Perdew and Wang[3] seems to be the most successful. This functional is a generalized gradient approximation (GGA) and has several attractive features, such as that it obeys the sum rules of the exchange-correlation hole and satisfies many of the scaling relations for the exchange-correlation energy. GGA and other nonlocal functionals have been tested on a number of systems,[4,5] but, to our knowledge, no systematic study of the differences between GGA and LDA has yet been performed for lanthanide systems. With the present paper, we intend to fill this gap by studying the equilibrium volumes, the bulk moduli, and the generalized cohesive energies, defined below, of the lanthanide elements using the LDA in the Hedin-Lundqvist parametrization[6] and the GGA by Perdew and Wang.[3]

It has been shown that the atomic-spheres approximation (ASA) affects the cohesive properties by approximately the same amount as the corrections introduced through GGA.[5] We therefore test the functionals together with a full-potential method, so that our results will be free of errors originating from shape approximations, thus only reflecting the limitations of the tested functionals.

The cohesive properties of the lanthanides, using an *ab initio* approach, have previously been calculated by Skriver[7]

and Min *et al.*[8] Cohesive energies of some lanthanides have also been calculated by Eriksson, Brooks, and Johansson.[9] All these calculations were performed using the LDA and the ASA. More recently, Melsen *et al.*[10] calculated the cohesive energies for all lanthanides in the LDA, using a full-potential approach. The crystal structure variation through the series was considered by Johansson and Rosengren,[11] and by Duthie and Pettifor.[12]

The rest of this Introduction is devoted to a short summary of some basic properties of the lanthanide series, relevant for the interpretation of our results.

The lanthanide series is generally considered to consist of the elements from La with atomic number 57 up to Lu with atomic number 71. This series is characterized by a gradual filling of the $4f$ shell. Since, in most cases, the $4f$ electrons are chemically inert and atomiclike, all lanthanides behave in a very similar manner and basic properties such as the atomic volume, bulk modulus, and melting temperature vary in a more or less regular manner across the series.[13] The assumption of an inert $4f$ shell is often called the standard model of the lanthanides. As the $4f$ shell is filled, the volume slowly decreases. This phenomenon is called the lanthanide contraction and mirrors the relatively passive role of the $4f$ electrons. To a large extent, they do not contribute to the bonding, and provide only a shielding of the nucleus and electron core. As the atomic number increases, the shielding becomes more and more incomplete since only the part of the $4f$ orbitals residing inside the valence orbitals can contribute to the screening, combined with the fact that the tail of the $4f$ orbitals outside the valence orbitals grows larger with increasing number of $4f$ electrons. The result is a contracted valence electron charge and thus smaller volume. Note that this picture neglects the nonsphericity of the $4f$ shell. This shell is spherically symmetric only for La, Gd, and Lu. Generally, the nonsphericity should give rise to small kinks in the lanthanide contraction.

In metallic form, all lanthanides are trivalent except Eu and Yb. If these two elements were to be trivalent, they would have had 6 and 13 electrons in the $4f$ shell, respectively, i.e., lacking one electron from having a half-filled $4f$ shell (Eu) or filled $4f$ shell (Yb). With a divalent valence configuration, the $4f$ majority-spin shell is filled for Eu, and for Yb the entire $4f$ shell is filled. This results in an energetically more favorable electron configuration. At ambient conditions all lanthanides except Eu crystallize in close-packed structures that differ only in their stacking sequences: fcc, hcp, dhcp, and Sm-type. The two latter structures, dhcp and Sm-type are intermediate between fcc and hcp. The early lanthanides La, Pr, Nd, and Pm crystallize in the dhcp phase, where the hexagonal layers are stacked in a way that can be described as halfway between hcp and fcc stacking. Throughout this paper, the calculations are performed in the fcc and hcp structures only. We tested this approximation on Pr, and found that the effects of more complicated stacking sequences were very minor, and that the results were intermediate in between those of fcc and hcp.

The late trivalent lanthanides all crystallize in the hcp phase. Sm has a unique and complicated rhombohedral structure, in which the stacking sequence is 2/3 hcp-like and 1/3 fcc-like. The c/a ratio is close to ideal in all these structures, although for the elements beyond Gd, the c/a ratio decreases somewhat.[14] Eu and Ba, which are divalent, crystallize in the bcc structure and Yb, also divalent, is fcc. Ce crystallizes in the fcc phase and has an isostructural phase transformation at elevated pressure with α-Ce as the low-temperature high-density phase and γ-Ce as the room-temperature low-density phase.[15] Throughout this paper, we will compare our calculated Ce results to experimental data for γ-Ce. The reason is that it is generally agreed upon that this phase of Ce metal has the $4f$ electron localized, i.e., the standard model of the lanthanides is applicable, whereas the situation for the $4f$ electron in α-Ce is a matter of controversy.[16]

The localized $4f$ shell gives rise to large local magnetic moments in the lanthanide series. Gd is ferromagnetic up to ambient temperature (24 °C), but the other lanthanides (except La, Yb, and α-Ce which are all nonmagnetic) have complicated magnetic structures in the ground state.[17] Even above the magnetic ordering temperature T_c, the large local moments affect the cohesive properties through local polarization of the valence and conduction bands.

II. DEFINITION OF THE GENERALIZED COHESIVE ENERGY

The cohesive energy E_{coh} is defined as the energy difference between the atomic and the bulk ground states. Experimentally, E_{coh} is deduced from thermochemical data. In contrast to the volume and bulk modulus, which vary more or less smoothly as a function of atomic number for the trivalent lanthanide metals, the cohesive energy exhibits an irregular behavior as the lanthanide series is traversed. Most of the lanthanides that have a trivalent ground state in the condensed phase have a divalent atomic configuration. Thus, promotion of a $4f$ electron to the $5d$ band takes place during condensation. The atomic energy associated with this valence change is called the promotion energy $E_{f \to d}$, and it varies substantially from one element to another. Note that

$E_{f \to d}$ is the energy difference between the divalent and trivalent *atom*. It is thus a purely atomic property. The irregular behavior of $E_{f \to d}$ as a function of atomic number explains to a large extent the irregularities in E_{coh}.[18] La, Gd and Lu are trivalent both in the atomic and condensed states and therefore the promotional energy correction does not apply to them.

Even after the addition of $E_{f \to d}$ to E_{coh}, some irregularities remain. It has been shown[18] that these are in fact due to the $5d-4f$ intershell coupling energy of the trivalent atom. To understand why this is the only coupling energy that enters, let us consider the different coupling energies present in the atom and in the solid. The total coupling energy in the trivalent atom consists both of a $4f$ intrashell coupling energy and a $5d-4f$ intershell coupling energy. Neither $6s$ nor $6p$ electrons contribute to the coupling energies since these shells are full and empty, respectively. The difference in $4f-5d$ intershell coupling energy between the two configurations in the solid is negligible above the magnetic ordering temperature. (The effect of the $4f-5d$ coupling in the solid can be calculated in a straightforward way, but for simplicity this was omitted in the present study.) Furthermore, the $4f$ intrashell coupling is the same as in the isovalent atom. Thus, the coupling energy difference between the atom and the solid, here called $\Delta E_{coupling}$, is, to a very large extent, a purely atomic property just as is $E_{f \to d}$, and it has been determined by Johansson and Munck[18] for all lanthanides using a relativistic Hartree-Fock-Slater (HFS) method and experimental ionization and excitation energies.

With the two corrections $E_{f \to d}$ and $\Delta E_{coupling}$ we construct, for the trivalent lanthanide metals, a smoothly varying function given by

$$E^* = E_{coh} + E_{f \to d} + \Delta E_{coupling}, \qquad (1)$$

where E^* is called the generalized cohesive energy. Its theoretical value is easily calculated as the difference between the total energy of the spin-degenerate trivalent atomic and bulk ground states.

The reference values of E^*, to which we will compare our theoretical values, are not purely experimental quantities since the determination of $\Delta E_{coupling}$ involves atomic HFS calculations. However, the HFS atomic calculations are only used as an improvement over a linear interpolation between La and Lu. Therefore, the E^* values for the intermediate elements are somewhat dependent of the accuracy of this interpolation procedure. Nevertheless, E^* will be referred to as an experimental value in the rest of the paper.

Above, we have not discussed Eu and Yb, the only two lanthanides divalent both in the atomic and metallic states. The atomic configurations for these metals are $f^7 s^2$ and $f^{14} s^2$, respectively, and do not involve any coupling between two open shells as in the case of the trivalent atomic configurations. Therefore the cohesive energies for Eu and Yb are not complicated by atomic effects. The same is, of course, true for Ba.

III. DETAILS OF THE CALCULATIONS

In our present calculation we used the full-potential linear muffin-tin-orbital method.[19,20] The Kohn-Sham equations are solved for a general potential without any shape approxima-

tion, which is important in order to profit from the merits of GGA.[5] Space is divided into nonoverlapping spheres (called atomic or muffin-tin spheres) surrounding each atomic site, and an interstitial region. The basis functions used are energy-independent Bloch functions, whose construction is somewhat different within the atomic spheres and in the interstitial region. Together with the variational principle, this leads to the fact that the secular equations become linear in energy and reduce to generalized eigenvalue equations, which can be solved by diagonalization.

In the interstitial region, the charge density is slowly varying, and the natural basis is plane waves, or Hankel and Neumann functions. A basis function in the interstitial is therefore expressed as a Bloch sum of Hankel or/and Neumann functions, which in turn is represented as a Fourier series. Formally, a basis function in the interstitial is defined by the Bloch function of solutions to the spherical Helmholtz equation with nonzero kinetic energy κ^2, or a linear combination of such solutions for different kinetic energies. The Fourier representation of this basis function is taken from the Fourier series of a function matching the basis in the interstitial region but not inside the atomic spheres, a so-called pseudowave function.

Inside the atomic spheres, where the charge density varies rapidly, the basis functions are Bloch functions built up of radial functions times spherical harmonics. In the present calculation, the expansion in spherical harmonics is taken up to $l = 8$. The radial part of a basis function is constructed from the numerical solutions $\phi_L(E_\nu, r)$ of the radial Schrödinger equation in a spherical potential at the fixed energy E_ν and their energy derivatives $\dot{\phi}_L(E_\nu, r)$. Here, the index L stands for a collection of quantum numbers: the principal quantum number n, the orbital quantum number l, the azimuthal quantum number m, and the kinetic energy κ^2. Depending on the sign of κ^2, the function in the interstitial region is a Hankel function ($\kappa^2 < 0$) or a Neumann function ($\kappa^2 > 0$).

The expressions for the crystal wave functions in the atomic spheres are matched to the interstitial crystal wave function at the sphere boundaries so that the total crystal wave function becomes continuous and differentiable in all space.

The potential used for solving the radial Schrödinger equation above is obtained from the charge density by solving the Poisson equation. In the first iteration, this density is taken as overlapping atomic charge densities. A new charge density is then constructed from the eigenvectors obtained through the variational procedure, and a new solution is obtained. The procedure can then be repeated until some criterion for self-consistency is met.

We used the pseudocore $5p$ wave, and the valence $6s$, $6p$, $5d$, and nf waves, where $n = 4$ for Ba and La and $n = 5$ in all other cases, i.e., Ce–Lu. Thus, for La and Ba, the $4f$ states are included in the valence, whereas for the other elements, the $4f$ states are in the core. In order to get a good description of the interstitial region, we used two basis functions with different κ^2 for each set of quantum numbers nlm. The entire basis was treated within one energy panel, so that a single fully hybridizing basis was formed. We sampled the reciprocal space with 2197 **k** points in the full Brillouin zone for fcc and with 1183 **k** points for hcp. The **k** points were

sampled using the special **k**-point sampling method developed by Chadi and Cohen,[21] and Froyen.[22]

The electron core, treated fully relativistically, was recalculated in each iteration. The valence states were described scalar relativistically, i.e., the Darwin term and the relativistic correction to the kinetic energy were included, but the spin-orbit interaction, which doubles the size of the problem, was neglected. The lanthanides are quite heavy elements, and therefore it is expected that relativistic effects should be important for their electronic structure. However, since the valence band is much broader than the spin-orbit splitting, the error introduced by omitting the spin-orbit interaction for the valence electrons is negligible.

As already mentioned, we used the Hedin-Lundqvist parametrization of the local-density functional[6] and for the generalized gradient corrected functional we used the form recently developed by Perdew and Wang.[3]

For the elements Ba, Ce, and Eu–Lu, the calculations were performed assuming the crystal structure found at ambient conditions. For the early lanthanides La, Pr, Nd, Pm, and Sm the calculations were performed both in the fcc and hcp structures. The equilibrium volumes and bulk moduli were extracted from the calculated energy/volume data points by fitting them to the equation of Vinet et al.[23] This equation is often called the "universal equation of state." Virtually the same results were obtained by fitting to the Birch equation[24] or to the Murnaghan equation.[25] In the calculation of the bulk moduli, the c/a ratio was kept constant and the bulk modulus was calculated both at the experimental and ideal value of c/a.

IV. ESTIMATION OF SYSTEMATIC ERRORS

Our goal is to compare two approximations of the exact density functional, a comparison that will be distorted by a number of systematic errors, such as the effect of magnetic ordering, local magnetic moments, thermal expansion, crystal structure, and nonspherical $4f$ shells. Before presenting our results, we will therefore discuss these sources of error.

The experimental volumes and bulk moduli quoted here (see Refs. 14 and 26, respectively) were measured at ambient temperature and pressure. Thermal expansion will therefore give a systematic error in our comparison with $T = 0$ theoretical data. For the volumes, we expect this effect to be very small, but for the bulk moduli, it could be more substantial. Of course, we could also have chosen to compare our results to 0-K data, but if we do that, we fall into the trap of having to correct for effects caused by complicated magnetic structures. The general trend in the experimental data can then not be expected to be smooth, which would obscure the interpretation of our calculations.

In order to estimate the temperature effect, we calculated the thermal expansion starting from the expression[27] for the thermal expansion coefficient α: $\partial V / \partial T = 3 \alpha V$, where V is the volume and T is the absolute temperature. In the present rough estimation we will assume that α is approximately constant over the relevant temperature range, i.e., from 0 K to ambient temperature, and that it is reasonable to use room-temperature values for α. The volume at temperature T, $V(T)$, is then given by

$$V(T) = V(0)(1 + 3 \alpha T), \qquad (2)$$

where $V(0)$ is the equilibrium volume at 0 K. At room temperature, α is approximately 7×10^{-6} K^{-1} for the trivalent lanthanides and about 30×10^{-6} K^{-1} for the divalent lanthanides.[14] This gives a volume thermal expansion of less than 1% for the trivalent and less than 3% for the divalent lanthanides.

To find the effect of thermal expansion on the bulk modulus we use the Murnaghan equation, according to which the bulk modulus scales with the volume as

$$B(V) = B(V_0) \left(\frac{V_0}{V} \right)^{B'_0}, \tag{3}$$

where B'_0 is the pressure derivative of the bulk modulus. This parameter is obtained directly in the Murnaghan fit to the energy-volume points. Using our calculated thermal volume expansion and the B'_0 values from the fit, we find that at room temperature, the bulk modulus is approximately 3% lower than at 0 K for the trivalent lanthanides. The corresponding value for the divalent lanthanides is 8%. The cohesive energy was negligibly affected by the thermal expansion.

Another possible source of systematic errors is the magnetic moment. Spin polarization of the bonding $5d$ electrons will cause less bonding states to become occupied, so we expect the volume to increase and, consequently, the bulk modulus to decrease. Even above the magnetic ordering temperature, where the moments are disordered, some of this effect will remain. In order to estimate the maximum value of this effect, we calculated the volume difference between non-spin-polarized Gd and Gd with a spin-polarized $4f$ core shell. It was found that the effect of the local magnetic moment was to expand the volume by 3% and decrease the bulk modulus with 19%. In the case of disordered moments above the magnetic ordering temperature, the effect should diminish since the $5d$ electrons then feel nonaligned moments from several atoms. Nevertheless, the effect of spin-polarized core electrons on the bulk modulus is definitely not negligible. In contrast, we found that the change in the cohesive energy due to the spin-polarized core was small, only around 0.01 eV.

The local magnetic moments should also have an effect on the general trend in the volumes and bulk moduli. It is reasonable to expect that the magnetic volume expansion is small early and late in the series, and has a maximum in the middle. This would result in a flatter trend for the early lanthanides and a more steep trend for the elements from Tb to Lu. For the bulk moduli, the effect on the trend would be the same as for the volumes, since the bulk moduli increase with atomic number and the local magnetic moments give a maximum decrease for Gd and no effect for La and Lu.

An error is also introduced by approximating the structures for the early lanthanides La, Pr, Nd, Pm, and Sm, which have complicated hexagonal crystal structures with longer period of the stacking sequences than hcp. In the calculations, these crystal structures have been approximated by hcp. In order to estimate the error introduced by this procedure, we compared the results from fcc and hcp calculations. It was found that the fcc volumes were typically 2% larger than the hcp volumes. The theoretical equilibrium volumes for the dhcp and Sm-type structures, which are the correct structures early in the series, are expected to fall in between the volumes for fcc and hcp, since they are intermediate regarding the stacking sequence. The crystal-structure error in the generalized cohesive energies was found to be around 0.05 eV. The effect of crystal structure on the bulk moduli for the early elements turned out to be small.

Next, we address a problem encountered when calculating the bulk modulus of a noncubic structure. Ideally, all degrees of freedom in the crystal structure should be relaxed in the calculation of the bulk modulus. However, such a procedure quickly becomes very time consuming especially if it has to be performed for many different systems. The error introduced by keeping the c/a ratio constant in the present calculations was estimated by performing the full, c/a relaxed calculation for one element in the series, Ho. For this element, we found that relaxing c/a made the value of the bulk modulus increase by 3%, i.e., the effect seems to be rather small.

Finally, an error is introduced by treating the partially filled $4f$ shells as spherical. Very recently, Brooks *et al.*[28] introduced a new way of calculating crystal-field energy levels using DFT. A central idea in their method is to perform ground-state calculations with nonspherical $4f$ core shells. We tested the effect of a nonspherical $4f$ core shell on Pr, using the method developed by Brooks *et al.*, and found the effect on the total energy negligible.

To summarize, the largest systematic errors are due to thermal expansion and magnetism. For the bulk moduli, the crystal structure is also of importance. The experimental volumes should in principle be shifted down a few percent to simulate paramagnetic 0-K results, and the experimental bulk moduli should be shifted up, whereas no shift is necessary for the generalized cohesive energies. Note that we have not actually performed these shifts of the experimental points.

V. RESULTS AND DISCUSSION

Our LDA and GGA results for the volumes of the lanthanides are shown in Fig. 1(a), together with the experimental volumes. The calculations were performed assuming the experimental crystal structures, with the exception that the dhcp and Sm-type structures were approximated with hcp. Thus, Ba and Eu were calculated in the bcc structure, Ce and Yb in the fcc structure, and all other elements were calculated in the hcp structure assuming the experimental c/a ratio. We see that for all elements having either an empty or full $4f$ shell, i.e., Ba, La, Yb, and Lu, the GGA results are in excellent agreement with experiment, whereas the LDA results underestimate the volumes by approximately 15%. For the early elements from Ce up to Pm, the LDA volumes appear to agree better with experiment than do the GGA volumes. For the later lanthanides, the GGA calculations again give excellent agreement with the experimental volumes. If the systematic errors discussed in the previous section were to be taken into account, we would have to shift down the experimental curve by a few percent, and Gd a little more. This would decrease somewhat the overestimation done by LDA. However, the shift is so small, that it would be barely visible on the scale of Fig 1(a).

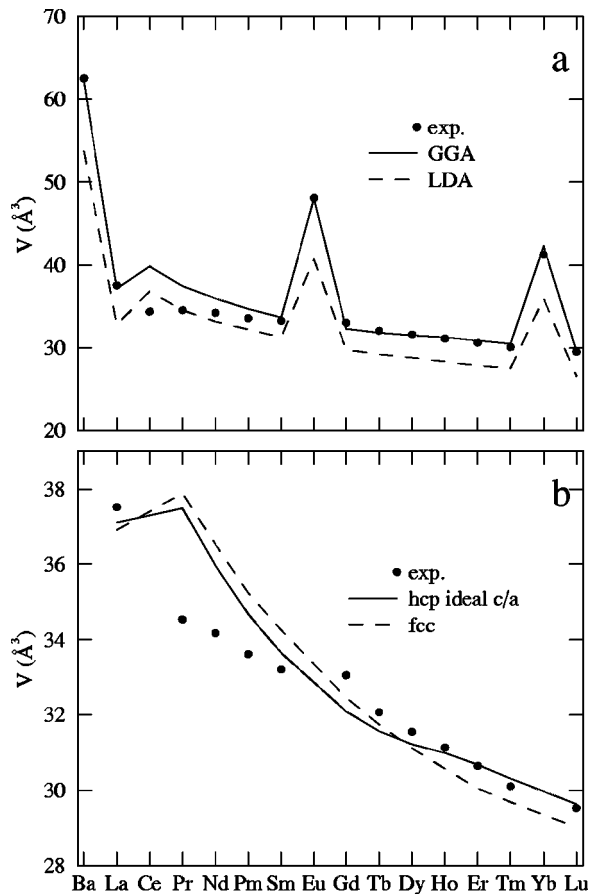For all elements studied here, GGA gives an upward shift

FIG. 1. (a) Experimental volumes at ambient temperature (taken from Ref. 14) and calculated volumes using LDA and GGA. Ba and Eu are calculated in the bcc structure, Ce and Yb in the fcc structure. All other elements are calculated in the hcp structure assuming the experimental c/a ratio. (b) Experimental volumes as above compared to calculated equilibrium volumes for two different crystal structures: hcp with ideal c/a ratio and fcc, for all trivalent lanthanides except Ce.
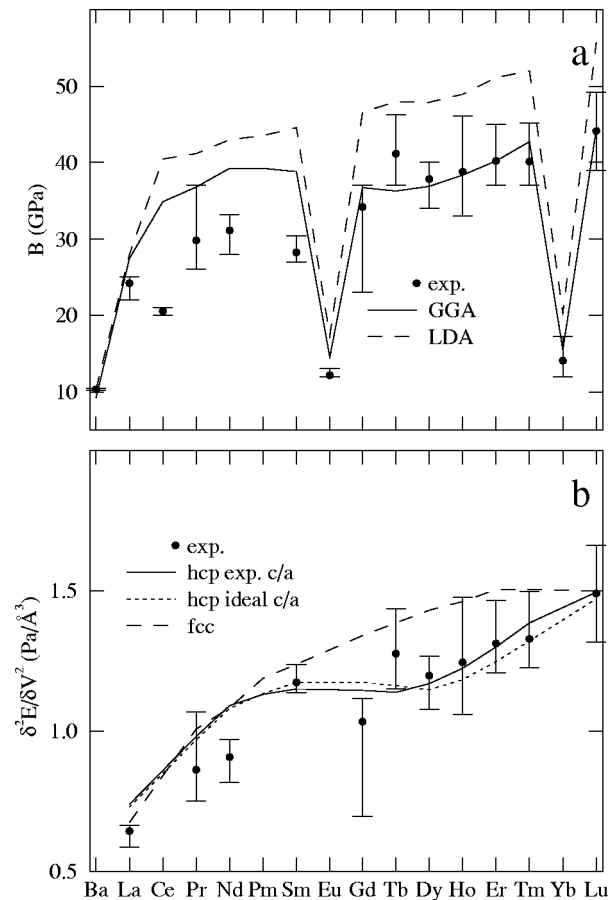
FIG. 2. (a) Experimental bulk moduli at ambient temperature (taken from Ref. 26) and calculated bulk moduli (evaluated at the theoretical equilibrium volume) for both LDA and GGA. Ba and Eu are calculated in the bcc structure, Ce and Yb in the fcc structure. All other elements are calculated in the hcp structure assuming a c/a ratio fixed at its experimental equilibrium value. (b) Calculated second energy derivative with respect to volume (evaluated at the theoretical equilibrium volume) for the trivalent lanthanides except Ce compared to experimental values calculated using the bulk moduli in Ref. 26 and volumes in Ref. 14.

in the equilibrium volume relative to LDA. The relative increase is largest for the divalent elements, where it is between 15% and 20%. For the trivalent elements, the shift is largest at both ends of the series, around 12%, and smaller in the middle, with a shift of only 7% for Sm.

Maybe more interesting than the absolute values of the volumes, is the way in which the volumes decrease as the series is traversed. Clearly, the calculations overestimate the lanthanide contraction for the early elements. This trend is the same both for LDA and GGA. The result of this erroneous trend is that LDA appears to give better results for the early elements from Ce and onwards. This, however, is a result of cancellation of errors and tells us that the error in the standard model of the lanthanides is about as large as the overbonding tendency of LDA, but with the opposite sign. Of course, as explained in the previous section, magnetism contributes to making the experimental trend flatter for the early lanthanides. This effect, however, is very small and cannot explain the discrepancy between the experiment and the calculation. Thus, our present implementation of the standard model of the lanthanides seems to be unsatisfactory for the early elements starting from Ce, in the series.

The crystal structure will affect the equilibrium volumes.

In Fig. 1(b) we compare calculations assuming the fcc structure to calculations performed in the hcp structure with ideal c/a ratio. Throughout, the GGA functional was used here. For the early lanthanides, the fcc structure gives larger volumes than the hcp structure, whereas for the later lanthanides, the situation is reversed. The effect on the volumes when changing the c/a ratio from the experimental to the ideal value was found to be rather small, and is therefore not shown. In Fig. 1(b), it becomes clearly visible that the experimental volume of Gd is abnormally large. This may to some extent be related to the fact that the volume was measured close to the Curie temperature, which is 24 °C for Gd.[14]

Figure 2(a) shows experimental and calculated (at the theoretical volume) bulk moduli, comparing the results from the two functionals. The crystal structures assumed are the same as in the volume calculations shown in Fig. 1(a), i.e., the calculations were performed with fixed c/a ratio. However, before discussing these results, we should say something about the experimental uncertainties in the bulk modulus.

In the literature, many different experimental values for

the bulk modulus can be found, and they differ substantially from one another. Grosshans and Holzapfel[26] have compiled a summary of measurements made on the lanthanides up to 1991 of both the adiabatic and isothermal bulk moduli. The experimental bulk moduli in Fig. 2(a) are calculated as the mean of the quoted isothermal bulk moduli, B_T, measured at room temperature, for each element and the error bars indicate the maximum and minimum measured values of B_T in their list. The value for Ba is taken from Kittel[29] and lacks error bars. The large lower error bar for Gd is probably due to the high Curie temperature for this element. Recall that our estimation of the decrease in the bulk modulus due to magnetism for Gd was 19%. Regarding the other systematic errors, not related to magnetism, estimated in the previous section, we note that the general experimental uncertainty in the bulk modulus seems to be much larger.

The first thing to note is that LDA overestimates the bulk modulus in all cases except for Ba. However, the nice result for Ba is due to cancellation of errors since, at the same time, LDA underestimates the equilibrium volume by approximately 15%. The average LDA overestimate of the bulk modulus, Ba excepted, is around 30% compared to the mean experimental values. This is qualitatively consistent with the result that LDA generally underestimates the volumes since a decrease in B is generally correlated to an increase in V, due to the softening of the lattice as it expands. The GGA results agree much better with experiment, also for the early lanthanides starting with Ce. In fact, for the elements beyond Sm, the agreement is excellent. This remains valid even after taking the effect of thermal expansion into account. Also, the agreement is very good for the elements having a closed $4f$ (sub)shell. For the early elements, GGA overestimates the bulk modulus. Naively, one would have expected the opposite, since GGA overestimates the volumes for these elements. This indicates, again, that our implementation of the standard model of the lanthanides breaks down for the early lanthanides from Ce and onwards.

A most interesting result regarding the trend in the bulk modulus emerges from our calculations. The trend in the GGA results resembles a third degree polynomial, with a local maximum in Nd and a local minimum in Tb. Note, that this trend is not observed in the LDA results.

In order to investigate this peculiar trend in the GGA results in more detail, we examined the second volume derivative of the total energy. In Fig. 2(b) we have plotted the second energy derivative with respect to volume, evaluated at the theoretical equilibrium volume, for three different crystal structures. The experimental points are the experimental bulk moduli divided by the experimental volumes. Note that the trend in the hcp calculations is completely different from the trend predicted when the fcc structure is assumed. For the late lanthanides, the agreement between the hcp calculations and experiment is excellent, whereas most of the fcc results are above the ends of the error bars of the experimental points. Best agreement is found for the hcp calculations with experimental c/a. The bend in the trend of the bulk moduli appears to be supported by experiment. We speculate that the origin of this bend has to do with changes in the Fermi surface. This aspect will be examined further in a future communication. For the early elements, all three crystal structures give very similar results.
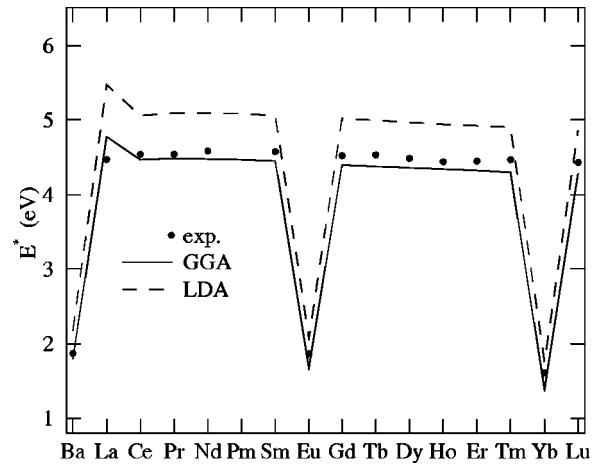

FIG. 3. Calculated generalized cohesive energies compared to experimental values taken from Ref. 18.

Finally, the generalized cohesive energies are presented in Fig. 3. Also here, GGA gives overall better results than LDA. The agreement between GGA and experiment for the elements with closed $4f$ (sub)shell is less satisfactory than for the volumes and bulk moduli. For Eu and Yb, the experimental points are placed almost intermediate in between the calculated LDA and GGA points, and for La both LDA and GGA overestimate the generalized cohesive energy, which is a unique situation. In contrast to the situation in La, the agreement between GGA and experiment is truly excellent for Ba, which is reassuring since the same basis set is used both for Ba and La ($4f$ instead of $5f$). LDA overestimates E^* by about 10% or 0.5 eV for the trivalent elements and 0.2 eV for the divalent. With GGA the agreement is excellent for the early trivalent metals (starting with Ce) with discrepancies less than 0.1 eV. For the heavier trivalent elements GGA underestimates E^* by about 4% or 0.2 eV, which is slightly worse than for the early lanthanides from Ce and onwards. In the divalent case, GGA gives a too low value by about 0.2 eV, i.e., the same as for the the heavier trivalent elements. The trend in the experimental values for the generalized cohesive energies is very smooth, and this trend is excellently reproduced by both LDA and GGA from Ce and onwards.

The theoretical and experimental generalized cohesive energies exhibit a slight ''lanthanide contraction'' behavior for the trivalent metals starting at Pr. The effect is not large, only about 0.1 eV, and is due to a combined effect of valence-orbital contraction and decreased $5d$ occupation as the series is traversed.

VI. CONCLUSIONS

In conclusion, our calculations show that for the elements studied here, GGA gives generally better volumes, bulk moduli, and cohesive energies than LDA. In fact, for the late lanthanides, the agreement is excellent for all properties studied. This is still true after taking thermal expansion, magnetic ordering, and approximated crystal structure, i.e., the most important systematic errors, into account. In principle, it would be most surprising if GGA were not to give better results than LDA, since GGA is explicitly constructed to be a more precise approximation to the true density func-

tional. On a more technical level, GGA gives better results since the nonlocality of exchange and correlation, which must become increasingly important for larger density variations, is better taken into account with this functional than with LDA. The effect is that GGA favors nonspherical densities more than LDA, and this results in larger lattice constants, since expansion increases the inhomogeneity. A larger lattice parameter, in turn, will lower both the bulk modulus and the cohesive energy. This argument, however, does not explain the difference between LDA and GGA in the trend in the bulk modulus.

The combination of GGA and a full-potential method resolves that the standard model of the lanthanides, in which the $4f$ complex is isolated from the valence states, is not satisfactory for the earlier elements (except, of course, La) in the lanthanide series. This is most easily seen in the trend of the experimental volumes, which for the early lanthanides, from Ce and onwards, is different from theory. Furthermore, LDA and GGA give different trends in the bulk modulus. The LDA trend is rather straight, whereas the GGA trend, which seems to be supported by the experimental points, resembles a third-order polynomial with a local maximum at Nd and a local minimum in Tb. This trend is not present in the calculations where the fcc structure was assumed. Thus,

both the crystal structure and the density functional is important in describing the trend in the bulk modulus of the lanthanides. This conclusion is consistent with previous work on the transition metals and the actinides.[4,5] The unusual trend in the observed bulk modulus and B/V ratio is most likely due to a rather intricate effect, not caused by, for instance, changes in the $5d$ occupation number or other concepts that previously have been successful in explaining the cohesive properties of the lanthanides.[7–9,12] We draw this conclusion based on the fact that theory reproduces this effect only when GGA in employed.

ACKNOWLEDGMENTS

[1] P. Hohenberg and W. Kohn, Phys. Rev. **136**, B864 (1964).

[2] W. Kohn and L. J. Sham, Phys. Rev. **140**, A1133 (1965).

[3] J. P. Perdew, in *Electronic Structure of Solids 1991*, edited by P. Ziesche and H. Eschrig (Akademie Verlag, Berlin, 1991), Vol. 11; see also http://camchem.rutgers.edu/~kieron/dft_pubs.html

[4] A. Dal Corso, A. Pasquarello, A. Baldereschi, and R. Car, Phys. Rev. B **53**, 1180 (1996); J. P. Perdew *et al.*, *ibid.* **46**, 6671 (1992); M. Körling and J. Häglund, *ibid.* **45**, 13 293 (1992); P. Söderlind, O. Eriksson, B. Johansson, and J. M. Wills, *ibid.* **50**, 7291 (1994); P. Söderlind, B. Johansson, and O. Eriksson, *ibid.* **52**, 1631 (1995); R. Ahuja *et al.*, *ibid.* **50**, 11 183 (1994); A. Khein, D. J. Singh, and C. J. Umrigar, *ibid.* **51**, 4105 (1995).

[5] V. Ozoliņš and M. Körling, Phys. Rev. B **48**, 18 304 (1993).

[6] L. Hedin and B. I. Lundqvist, J. Phys. C **4**, 2064 (1971); U. von Barth and L. Hedin, *ibid.* **5**, 1629 (1972).

[7] H. Skriver, in *Systematics and the Properties of the Lanthanides*, edited by S. P. Sinha (Reidel, Dordrecht, 1983), p. 213.

[8] B. I. Min, H. J. F. Jansen, T. Oguchi, and A. J. Freeman, J. Magn. Magn. Mater. **61**, 139 (1986).

[9] O. Eriksson, M. S. S. Brooks, and B. Johansson, J. Less-Common Met. **158**, 207 (1990).

[10] J. Melsen, J. M. Wills, B. Johansson, and O. Eriksson, J. Alloys Compd. **209**, 15 (1994).

[11] B. Johansson and A. Rosengren, Phys. Rev. B **11**, 2836 (1975).

[12] J. C. Duthie and D. G. Pettifor, Phys. Rev. Lett. **38**, 564 (1977).

[13] B. Johansson and M. S. S. Brooks, in *Handbook on the Physics and Chemistry of the Rare Earths*, edited by K. A. Gschneidner, Jr., L. Eyring, G. H. Lander, and G. R. Choppin (North-Holland, Amsterdam, 1993), Vol. 17, Chap. 112, p. 149.

[14] K. A. Gschneidner, Jr., Bull. Alloy Phase Diagrams **11**, 216 (1990).

[15] D. C. Koskenmaki and K. A. Gschneidner, Jr., in *Handbook on the Physics and Chemistry of the Rare Earths*, edited by K. A.

Gschneidner, Jr. and L. Eyring (North-Holland, Amsterdam, 1978), Vol. 1, Chap. 4.

[16] B. Johansson, Philos. Mag. **30**, 469 (1974); J. W. Allen and R. M. Martin, Phys. Rev. Lett. **49**, 1106 (1982); J. W. Allen and L. Z. Liu, Phys. Rev. B **46**, 5047 (1992); A. Svane, Phys. Rev. Lett. **72**, 1248 (1994); Z. Szotek, W.M. Temmerman, and H. Winter, *ibid.* **72**, 1244 (1994); B. Johansson *et al.*, *ibid.* **74**, 2335 (1995); J. M. Wills, O. Eriksson, and A. M. Boring, *ibid.* **67**, 2215 (1991); A. M. Boring, R. C. Albers, O. Eriksson, and D. D. Koelling, *ibid.* **68**, 2652 (1992).

[17] See, e.g., *Systematics and the Properties of the Lanthanides*, edited by S. P Sinha (Reidel, Dordrecht, 1983).

[18] B. Johansson and P. Munck, J. Less-Common Met. **100**, 49 (1984); B. Johansson, Phys. Rev. B **20**, 1315 (1979).

[19] J. M. Wills (unpublished); J. M. Wills and B. R. Cooper, Phys. Rev. B **36**, 3809 (1987); D. L. Price and B. R. Cooper, *ibid.* **39**, 4945 (1989).

[20] O. K. Andersen, Phys. Rev. B **12**, 3060 (1975); H. L. Skriver *The LMTO Method* (Springer, Berlin, 1984).

[21] D. J. Chadi and M. L. Cohen, Phys. Rev. B **8**, 5747 (1973).

[22] S. Froyen, Phys. Rev. B **39**, 3168 (1989).

[23] P. Vinet, J. Ferrante, J. R. Smith, and J. H. Rose, J. Phys. C **19**, L467 (1986); P. Vinet, J. H. Rose, J. Ferrante, and J. R. Smith, J. Phys.: Condens. Matter **1**, 1941 (1989).

[24] F. Birch, Phys. Rev. **71**, 809 (1947).

[25] F. D. Murnaghan, Proc. Natl. Acad. Sci. USA **30**, 244 (1944).

[26] W. A. Grosshans and W. B. Holzapfel, Phys. Rev. B **45**, 5171 (1992).

[27] N. W. Ashcroft and D. N. Mermin, *Solid State Physics* (Saunders College, Philadelphia, 1976), p. 492.

[28] M. S. S. Brooks, O. Eriksson, J. M. Wills, and B. Johansson, Phys. Rev. Lett. **79**, 2546 (1997).

[29] C. Kittel, *Introduction to Solid State Physics* (Wiley, New York, 1976).